DC LIMITED ANGLE TORQUE ELECTRICAL MOTOR

Ioana IONICA[1], Mircea MODREANU[2], Alexandru MOREGA[3], Cristian BOBOC[4]

Numerical modeling has become a de facto tool in the design stage of electric machines. This paper presents two- and three-dimensional models aimed to develop a DC limited angle torque motor. These models are important for establishing the constructive solution of a DC limited angle torque motor.

Keywords: DC Limited Angle Torque Motor, numerical modeling, optimal design, finite element method

1. Introduction

The DC limited angle torque motor (DC-LATM) belongs to the category of brushless DC motors, and it is currently under development in the country and abroad [1]. This motor is mounted directly to the drive shaft (in a direct drive), without requiring additional mechanical transmission elements such as flexible couplings and gearboxes [2-4].

DC-LATM lacks the brush–collector system specific to classical DC motors therefore the pending mechanical friction torque is absent, and this recommends it for limited angle drives of high performance [5,6]. The absence of notches in the stator reduces the cogging torque to zero, thus ensuring a uniform torque-angle characteristic over the operating range [7-9].

The winding of the DC-LATM stator is toroidal, multilayered, either dipolar, for a large angular operating range, or multipolar, for a small angular operating range and a higher electromagnetic torque [9]. DC-LATMs are recommended for applications in which the volume and the weight of the system are critical.

Numerical and analytical models and results concerning DC-LATM make the object of a number of studies [10-15]. Building on these in order to improve the design of a DC-LATM motor, here, finite element numerical modeling is used from the design phase (Fig. 1) [16-18]. Two-dimensional and three-dimensional numerical models are used. First, 2D models account for those components only that matter

[1] Icpe - MESSICO Department, and Faculty of Electrical Engineering, University POLITEHNICA of Bucharest, Romania, E-mail: ioana.messico@icpe.ro
[2] Icpe - MESSICO Department, Romania, E-mail: mircea.messico@icpe.ro
[3] Faculty of Electrical Engineering, University POLITEHNICA of Bucharest, Romania, E-mail: alexandru.morega@upb.ro
[4] Icpe - MESSICO Department, Romania, E-mail: cristianboboc.messico@icpe.ro

from the electromagnetic point of view, including the magnetic field sources: Samarium-Cobalt magnets situated on the rotor and the currents in the coils [19]. Next, 3D models are introduced with the aim to overcome several inconsistencies that are observed between the numerical model and the physical experiments when 2D models are used.

2. Mathematical model for the magnetic field in the DC-LATM

We consider only the components that matter from the electromagnetic point of view and chosen stationary working conditions. Then, the physical model is made of the

Magnetic circuit law

$$\nabla\times\mathbf{H}=\mathbf{J}, \tag{1}$$

Magnetic flux law

$$\nabla\cdot\mathbf{B}=0, \tag{2}$$

Constitutive law

$$\mathbf{B}=\mu_0\mu_r\mathbf{H}+\mathbf{B}_r\ . \tag{3}$$

Here, **H** [A/m] is the magnetic field strength, **J** [A/m^2] is the current density, **B** [T] is magnetic flux density, $\mathbf{B}_r$ [T] is the remanent magnetic flux density (within the permanent magnets), μ_0 [H/m] is magnetic permeability of vacuum, and μ_r is relative magnetic permeability. By (4), $\mathbf{B}=\nabla\times\mathbf{A}$, where **A** [T/m] is the magnetic vector potential. The boundary condition that closes the problem is magnetic insulation, $\mathbf{n}\times\mathbf{A}=0$ (**n** is the outer normal to the boundary).

The coils, with N turns, carry the electrical current I_{coil} [A]. The DC electrical current density is

$$J=\frac{N\cdot I_{coil}}{S}, \tag{5}$$

where S [m^2] is the cross-sectional area of the conductor in the coil.

3. Two-dimensional models

Different configurations for a DC-LATM were evaluated, out of which this paper presents two different designs with two different shapes for the magnets.

2D Model – Variant 1

Fig.1.a. shows the main parts of model used in numerical modeling: (1) the stator stack (electrotechnical sheet Iron Silicon – Iron M19); (2) the stator winding (Copper); (3) the air gap, (4) the permanent magnet (Sm_2Co_{17} 28H), and (5) the rotor shaft (Iron 416). Fig. 1.b. presents the B-H characteristics of the two ferromagnetic materials.

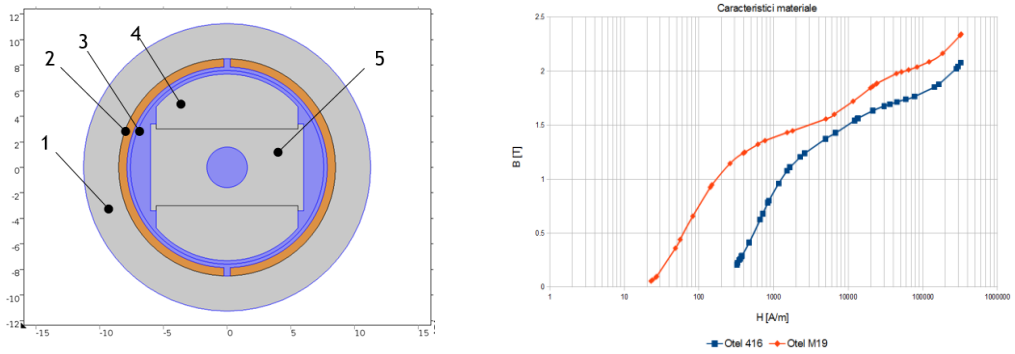

a. The constructive parts used in numerical modeling. Dimensions are in millimeters.

b. Materials B-H characteristics.

Fig. 1. Main parts of model used in numerical modeling and their magnetic properties.

Fig. 2 presents an example of unstructured FEM mesh, made of second order, Lagrange, triangular elements. The mesh in the air gap must be fine enough to provide for accurate numerical results.

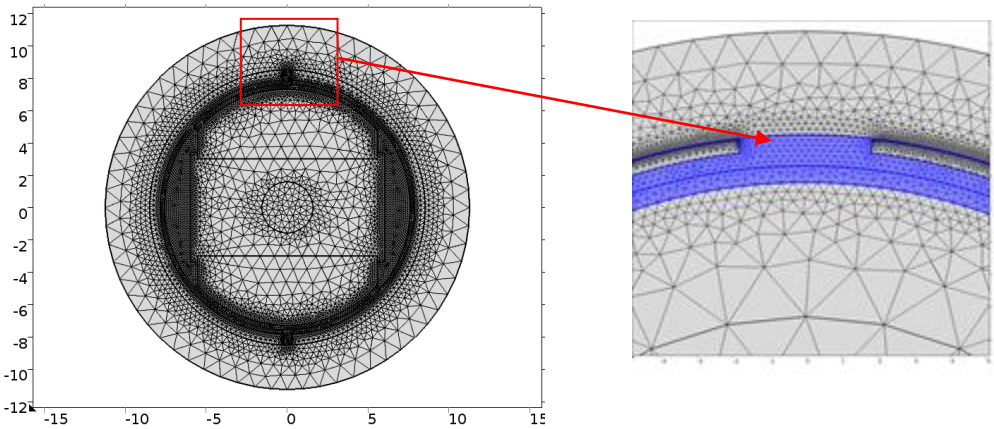

Fig. 2. The mesh used for numerical simulations. Dimensions are in millimeters.

Fig. 3 shows the magnetic flux density field (arrows) and the vector potential (contour lines with color proportional to the local value) computed using the finite element method (FEM) [7] to solve the problem (1)-(3).

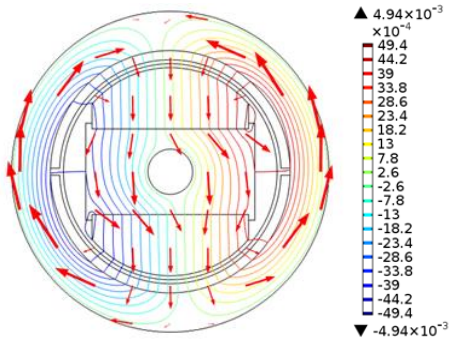

Fig. 3. The magnetic field: flux density (arrows) and vector potential (contour lines).

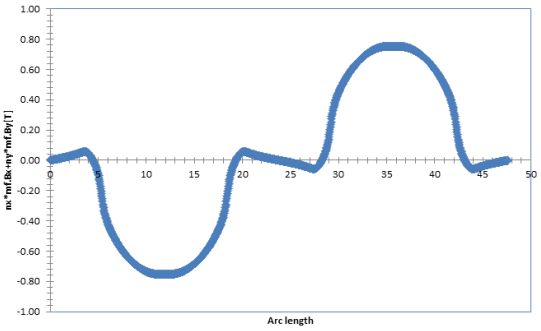

Fig. 4. The radial component of the magnetic flux density in the air gap.

Fig. 4 unveils the the radial component of the magnetic flux density in the air gap. The surface color map of magnetic flux density in Fig. 5 evidences certain sections of the stator that approach the saturation limit, without exceeding 1.46 T in the stator, and 1 T in the rotor yoke, acceptable for the chosen materials.

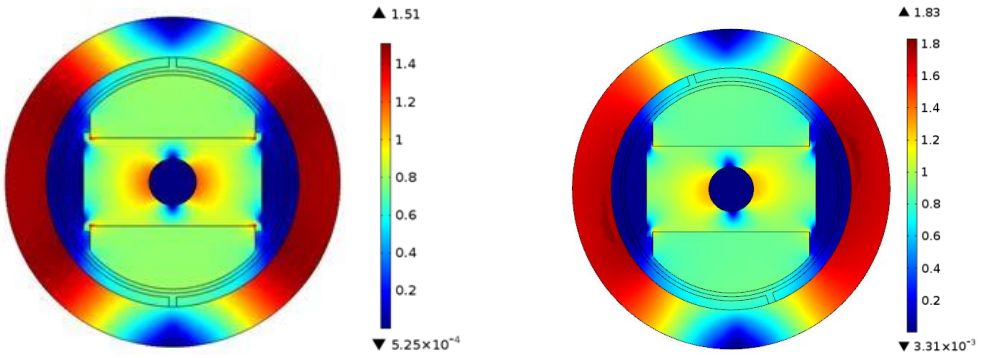

a. $\alpha = 0^o$ b. $\alpha = 20^o$

Fig. 5. Magnetic flux density for two rotor to stator angular positions – values are in tesla.

The values for magnetic flux density are acceptable for the chosen magnetic materials. The results presented are shown for only one case, at 180º. The worst case (from the saturation point of view) is obtained at 20º, as seen next.

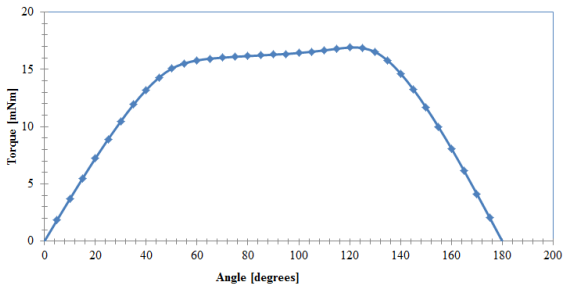

Fig. 6. Torque-angle characteristic.

The torque-angle characteristic in the 0÷180º range is depicted in Fig. 6. The maximum torque value is about 17 mNm, obtained at 125º.

2D Model – Variant 2

A different rotor design, using the same materials, is shown in Fig. 7.a.: (1) the stator stack; (2) the stator winding; (3) the air gap; (4) the magnet, and (5) the rotor shaft.

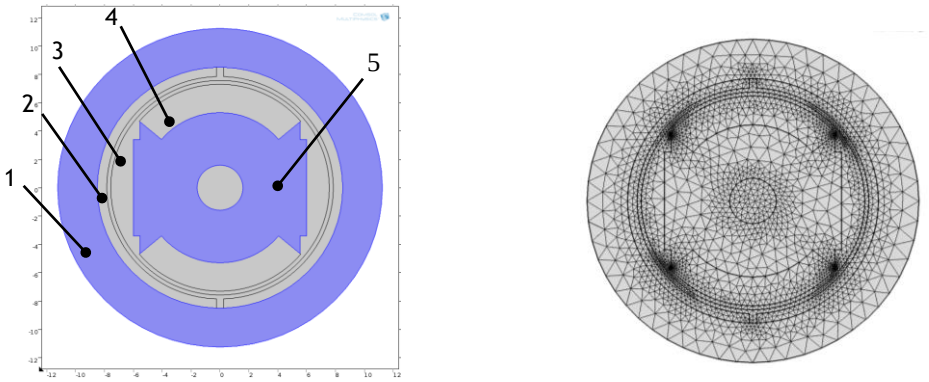

a. The constructive parts. b. The 2D FEM mesh.

Fig. 7. The constructive parts used in numerical modeling. Dimensions are in mm.

Fig. 7.b. presents an example of unstructured FEM mesh, made of second order Lagrange, triangular elements. Same mesh resolution concerns occur, and they are solved by using local refinements in the regions of steeper variations of the solution (the magnetic vector potential).

The magnetic flux density field (arrows) and the vector potential (contour lines with color proportional to the local value) (Fig. 8) clearly outline the fascicular magnetic flux density path in the motor.

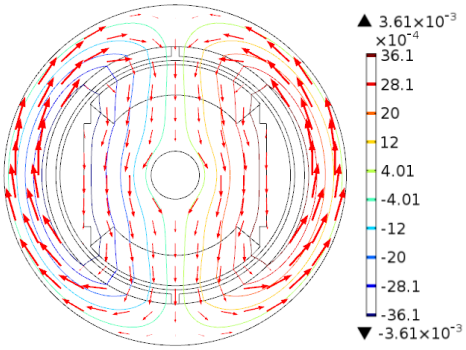

Fig. 8. The magnetic flux density (arrows) and magnetic vector potential, z component [Wb/m] (contour lines).

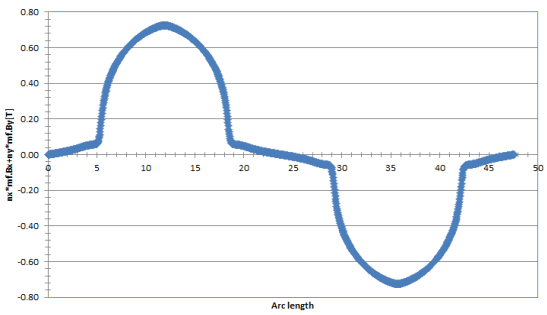

Fig. 9. The radial component of the magnetic flux density in the air gap.

The distribution of the radial component of the magnetic flux density in the air gap is rendered in Fig. 9, which shows off a maximum value of 0.7 T.

The surface color map of magnetic flux density (Fig. 10) indicates the sections in the stator that approach the saturation limit, *i.e.*, 1.48 T in the stator and 1.15 T in the rotor. The values are acceptable for the chosen materials however the magnetic flux density values are bigger than those in the previous design.

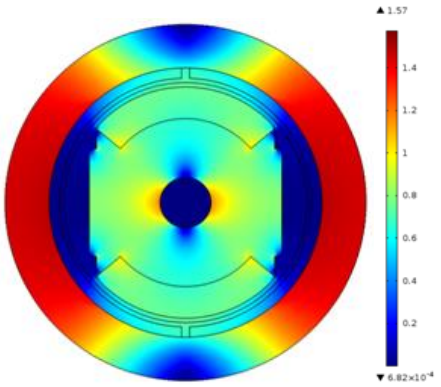

Fig. 10. Magnetic flux density – surface color map, values are in tesla.

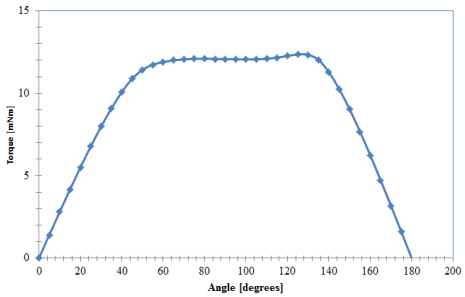

Fig. 11. Torque-angle diagram obtained out of the 2D model.

The torque-angle characteristic (Fig. 11) for the rotor to stator relative position within the 0÷180º rotational displacement range presents smaller values than those in Variant 1.

4. Three-dimensional modeling

Because some numerical results produced by 2D modeling are inconsistent with experimental measurements, we considered 3D modeling that may take into account a number of aspects that cannot be considered by 2D models. The rotor has different diameters. Thereby, was realized a 3D model, which will discard the simplifying assumptions used in 2D modeling. Fig. 13 present the constructive parts of model used in numerical modeling: (1) the stator stack; (2) the stator winding; (3) the air gap, (4) the magnet; (5) the rotor shaft, and (6) the air domain. For three-dimensional modeling we chose the first variant of 2D model because that produced bigger torque values.

The magnetic field problem is closed at finite distance (Fig. 12) using a containing, finite volume of air. The same magnetic materials are used. Fig. 13 presents the mesh used for numerical simulations. The mesh, made of tetrahedral elements, has to be fine enough in the air gap to provide for accurate numerical results.

Fig. 14 shows the magnetic flux density field (arrows) and the vector potential (contour lines with color proportional to the local value) that evidence

the magnetic field density paths and singles out the sections in the stator prone to saturation.

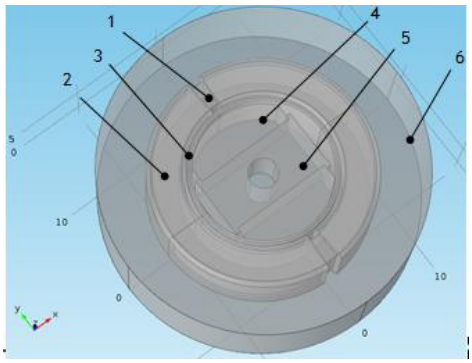

Fig. 12. The constructive parts used in numerical modeling. Dimensions are in mm.

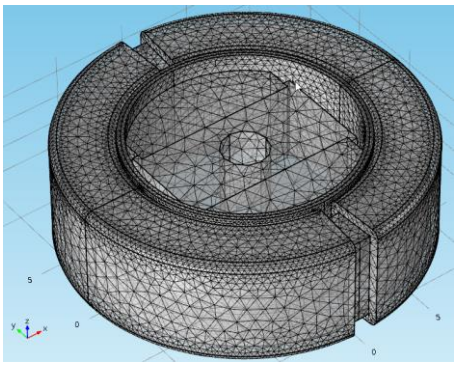

Fig. 13. The FEM mesh.

The magnetic flux density (surface color map in Fig. 15, values in tesla) reaches 1.4 T in the stator, which is acceptable for the chosen materials.

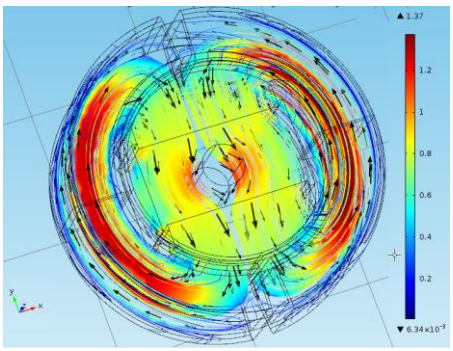

Fig. 14. The magnetic field: flux density (arrows) and vector potential (contour lines).

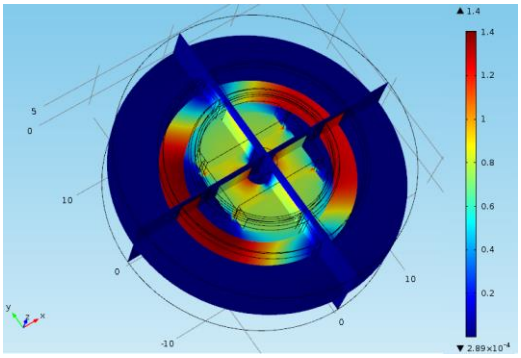

Fig. 15. Magnetic flux density – surface color map, values are in tesla.

The torque-angle diagram for rotor to stator rotational shift within the range 0÷180º is shown in Fig. 16.

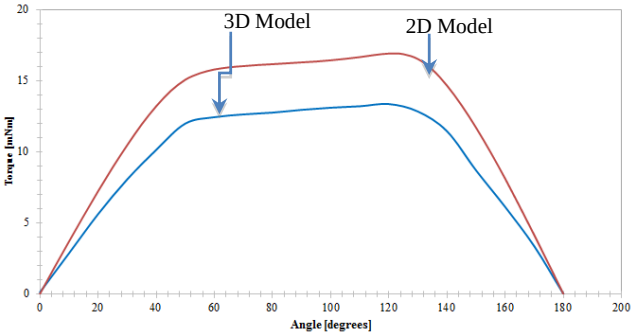

Fig. 16. The torque-angle diagrams obtained out of the 2D and 3D models.

The torque values are smaller than those produce by the bi-dimensional model (Fig. 6). A comparison of the two models is presented in Fig. 16.

This may be because the 2D models are based on simplifying assumptions, which presume that all parts of the model have the same length. These are discarded in the 3D models.

5. Conclusions

This paper aims to obtain torque-angle characteristics of the DC Limited Angle Electrical Motor with a small margin of error with respect to the experimental data. Using a finite element method (FEM), different configurations for a DC limited angle torque motor were evaluated. Two different configurations with magnets of different shapes are presented.

The two-dimensional models take into account simplifying assumptions, which presume that all components of the model have the same length. Therefore, the torque results are significantly higher than the measurements, the relative deviation on the operating range (-60º - +60º) at the position of maximum torque (0º) between numerical and experimental results being equal with 22.31%. The maximum relative deviation for two-dimensional approximation on the operating range is equal with 36.06% and it is at -60º.

The second, two-dimensional model produces smaller torque values than its 3D counterpart in the first variant.

Due to the fact that all components of the two-dimensional model have the same length, a three-dimensional model was used, which gives more accurate results. The maximum relative deviation on the operating range (-60º - +60º) at the position of maximum torque (0º) between numerical and experimental results is equal with 7.13%. The maximum relative deviation for three-dimensional model on the operating range is equal with 18.8% and it is at -+60º.

When compared with the two-dimensional model, the torque values for three-dimensional model are smaller, and they approximate better the

experimental data. The differences between the data of two-dimensional approximation, three-dimensional model and the experimental one, are due to the materials used in the numerical modelling process and in the experimental model.

The actual design gives experimental data that fulfill the requirements from customer Technical Specification. Nevertheless, based on the results obtained, for future design, an optimization concerning the transversal geometry may be taken into account.

R E F E R E N C E S

[1] *D. Stoia*, Excited DC motors with permanent magnets [in Romanian] (Motoare de curent continuu excitate cu magneţi permanenţi), Ed. Tehnică, București 1983.

[2] *P.R. Upadhyay, K.R. Rajagopal, B.P. Singh*, "Computer aided design of an axial-field permanent magnet brushless dc motor for an electric vehicle", in Journal of Applied Physics, **vol. 93**, no.10, May 2003, pp.8689-8691.

[3] *P.R. Upadhyay, K. R. Rajagopal*, "FE Analysis and Computer-Aided Design of a Sandwiched Axial-Flux Permanent Magnet Brushless DC Motor", in IEEE Transactions on Magnetics, **vol. 42**, no.10, Oct. 2006, pp. 3401-3403.

[4] *P.R. Upadhyay, K.R. Rajagopal*, "FE analysis and CAD of radial-flux surface mounted permanent magnet brushless DC motors", in Digests of the IEEE International Magnetics Conference – INTERMAG, 4–8 April 2005, pp.729-730.

[5] *R. Obreja, I.R. Edu*, "Limited Angle Torque Motors having high torque density, used in accurate Drive Systems", in Acta Polytechnica, **vol. 51**, no. 5, 2011, pp.75-83.

[6] *M.I. Andrei, N.M. Modreanu*, "Numeric Modelling of a Two-Channel Limited Angle Torque Motor" [in Romanian] (Modelarea numerică a unui motor de cuplu cu unghi limitat cu două canale), în EEA – Electrotehnică, Electronică, Automatică, Ed. ELECTRA, **vol. 62**, no. 1, 2014, pp. 26-31.

[7] COMSOL Multiphysics Documentation http://www.comsol.com/.

[8] Icpe, Electromechanical components for high-tech direct drive systems realized with flexible technology lines – HTDD [in Romanian] [Componente Electromecanice pentru Sisteme High Tech Direct Drive realizate cu Linii Tehnologice Flexibile - HTDD], etapa I, http://www.icpe.ro/htdd/ro, Oct. 2013.

[9] *R. Măgureanu*, Mașini electrice speciale pentru sisteme automate [in Romanian] (Special electrical machines for automatic systems), Ed. Tehnică, București, 1981.

[10] *M. Modreanu, A. Morega*, "Analiza numerică a fenomenelor electromagnetice și termice într-un motor de curent continuu de mică putere" [in Romanian] (Numerical analysis of electromagnetic and thermal phenomena in a low power DC motor), Sesiunea omagială de comunicări științifice "55 de ani de activitate a Grupului Icpe în dezvoltarea sectorului electrotehnic", Sept. 20 – 21, 2005, București.

[11] *M. Modreanu, M. Morega*, "Evaluarea numerică și experimentală a unui motor de curent continuu cu magneți permanenți" [in Romanian] (Numerical and experimental evaluation of a DC motor with permanent magnets), Simpozionul Actualități și Perspective în domeniul mașinilor electrice, Ediția a V-a, Universitatea POLITEHNICA din București, Catedra de Mașini, Acționări și Materiale, ISSN 1843-5912, 13 – 14 octombrie 2009.

[12] *T. Tudorache, M. Morega*, "Calculul 3D al încălzirii unui motor de c.c. de mică putere folosind metoda elementului finit" [in Romanian] (3D calculation of the heating of a low-power dc motor using the finite element method), Simpozionul Actualități și Perspective în domeniul mașinilor electrice, Ediția a V-a, Universitatea POLITEHNICA din București,

Catedra de Mașini, Acționări și Materiale, ISSN 1843-5912, 13 – 14 octombrie 2009.
[13] *O. Craiu, A. Machedon,* "3D finite element thermal analysis of a small power pm dc motor – optim", in 12th International Conference on Optimization of Electrical and Electronic Equipment, May 20–22, 2010, Brașov.
[14] *O. Craiu, A. Machedon*, "Modele electromagnetice și termice pentru servomotoare de c.c. cu magneți permanenți" [in Romanian] (Electromagnetic and thermal models for AC servomotors with permanent magnets), Tendințe de dezvoltare în fabricația mașinilor electrice și cerințe actuale ale UE, Universitatea Politehnica din București, 1 Aprilie, 2010.
[15] *O. Craiu, M. Modreanu*, "Studiu experimental și numeric al încălzirii unui motor de c.c. de mică putere, în condiții de funcționare variate" [in Romanian] (Experimental and numerical study of the heating of a low-power DC motor under various operating conditions), Simpozionul de mașini electrice SME 2010, 7 – 8 Octombrie, 2010, București.
[16] Icpe, Electromechanical components for high-tech direct drive systems realized with flexible technology lines – HTDD [in Romanian] [Componente Electromecanice pentru Sisteme High Tech Direct Drive realizate cu Linii Tehnologice Flexibile - HTDD], etapa II, http://www.icpe.ro/htdd/ro, Oct. 2013.
[17] *J.-M. Jin*, "The Finite Element Method in Electromagnetics", in John Wiley and Sons Publisher, New York, 2002.
[18] *M.I. Andrei, N.M. Modreanu, M. Guțu, L. Ghițulescu*, "Sistem de măsură asistat de calculator pentru caracterizarea motoarelor de cuplu cu unghi limitat" [in Romanian], (Computer Aided Measurement System for the Characterization of Limited Angle Torque Motors), in EEA - Electrotehnică, Electronică, Automatică, Ed. ELECTRA, **vol. 62**, no. 3, June-Sept., 2014, ISSN 1582-5175.
[19] *C. Ghiță*, Elemente fundamentale de mașini electrice [in Romanian] (Basic Elements of Electrical Machines), Ed. PRINTECH, București, 2002.